ISSN: 2414-1895 DOI: 10.6919/ICJE.202205_8(5).0090

Interference Alignment in Frequency-Domain Using Doppler Effect

Bisheng Liu[a], Feng Liu[*]

College of Information Engineering, Shanghai Maritime University, Shanghai, China

[a]201930310047@stu.shmtu.edu.cn, [*]liufeng@shmtu.edu.cn

Abstract

This letter investigates the implementation of perfect interference alignment (IA) in frequency-domain for 2×2 X channels, where each of the two source nodes sends two independent messages to each of the two destination nodes. The key is to change the frequency of the interference signal to ensure that it does not overlap with the desired signal. We propose an IA approach using the Doppler effect. The system consists of four access points, each of which has a circular drum antenna. The circular drum antenna is designed in such a way that it shifts the interfering signals away from the desired signal band. We give two specific schemes and their constraints, and prove their feasibility.

Keywords

Doppler Effect; Interference Alignment; Frequency Domain; X Channel.

1. Introduction

Nowadays, wireless network has completely changed people's life. Wireless networks typically consist of a collection of wireless transmitters and receivers, and use a fixed band of radio frequency (RF) spectrum for communication. Due to spectrum scarcity, wireless networks often reuse their limited frequency spectrum, which will cause the problem of inter channel interference. Recently, interference alignment (IA) has become an effective method to improve the accuracy and degrees of freedom (DoF) of information transmission. IA can effectively alleviate the interference in wireless networks. The key idea behind IA is to align interfering signals into the same subspace, while desired signals lie in orthogonal subspaces. The idea of IA can be implemented in time/frequency/space domains, separately or jointly. In this letter, we focus on IA in frequency domain, which utilizes frequency offset caused by the Doppler effect to align interference signals.

In [1], the authors proposed a new scheme based on IA, which realizes the total available DoF of K-user interference channel. Cadambe and Jafar are the first to prove that in a system with K interfering transmitter-receiver pairs, each pair gets more than a 1/K resource share, and the sum of all shares is larger than one. On this basis, the authors in [2] theoretically deduced the necessary and sufficient conditions for the feasibility of CJ-3U-IA scheme in three user SISO OFDM system and the feasibility of frequency domain IA is also proved. In time domain, the authors in [3] proposed a feasible scheme to achieve the DoF of K×2 XC based on propagation delay alignment (PDA) structure and the authors explore the PD feature among different links to maximize the achievable DoF with the minimum cost [4]. In spatial domain, all the channel transmitters cooperatively align by exploiting channel state information (CSI) at transmitters their transmissions in such a way that the interference subspaces at all the receivers jointly are limited to a smaller dimensional subspace, and are orthogonal to the desired signal subspaces [5]. In frequency domain, the author in [6] applied IA to inter vehicle communication, and can effectively ensure that there is no interference between vehicles through subcarrier coding. The authors in [7] proposed a novel IA algorithm which is combined with the

ISSN: 2414-1895 DOI: 10.6919/ICJE.202205_8(5).0090

sparse code multiple access (SCMA) technique can provide significant BER gain. In [8], the authors utilized specially designed alignment signals that can cancel the interference of one symbol on the other and add an additional signal component that makes the signal circularly convolved with the channel at the receiver side. IA can also be performed in space-frequency domain, e.g., the authors proposed a low complexity resource allocation scheme appropriate to both spatial and frequency domain IA [9].

Nowadays, most of the work on frequency domain focuses on subcarrier resource allocation. The goal of this paper is to investigate the IA in frequency domain by exploiting the Doppler effect. We introduce a new paradigm for wireless communication, namely Doppler assisted interference alignment (DAIA). We propose a rotating antenna to simulate the Doppler effect as shown in Fig.1, and change the receiving frequency band of the signal through the relative motion of the transmitting nodes and the receiving nodes.

Rotating Drum Antenna:

In [10], a rotating antenna suitable for microwave or millimeter wave (MMW) communication is presented, which can improve the anti-interference ability of communication line. In [11], the author developed a new rotating antenna, which can transmit RF signals to six different beams in receiving and transmitting modes. In [12], the author introduces a rotating wide slot antenna, which can meet the needs of modern communication technology to integrate various communication systems in a limited space. Nowadays, rotating antenna is widely used in Doppler feature extraction of UAV, Moreover, the rotating antenna can also assist wireless communication in interference alignment [13]–[15], Fig. 1-(a) illustrates the proposed circular drum antenna for DAIA. In order to simulate the Doppler effect, the circular antenna is rotating. The rotatable antenna is an omnidirectional antenna, and its radiation surface is located on the side of the cylinder for receiving and transmitting signals. Therefore, different link channel responses show different frequency characteristics. Of course, the most important influence is the rotation speed of the antenna. Despite Doppler effect being considered as an major impairment, the results in this paper indicate that The degree of freedom can also be increased by using Doppler effect.

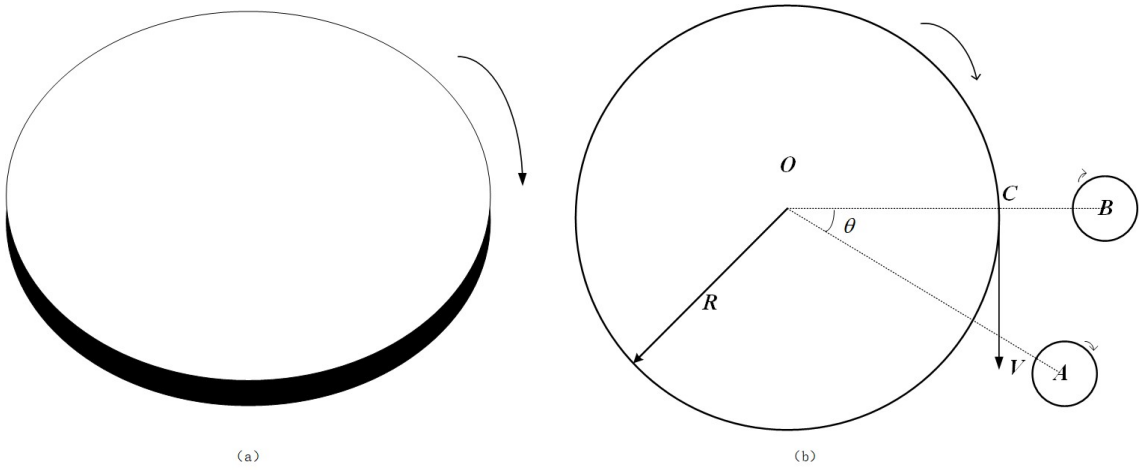

Fig. 1 (a) A possible antenna implementation of DAIA,which is an omnidirectional rotating antenna with a signalradiation surface on its side; (b) the top view of the rotating antenna

Rotating antenna is used in military field and satellite communication field, such as TACAN (for tactical air navigation) system, The TACAN system has multiple antennas installed in a circle, and electronically steers a radio beam in order to provide directional information for distance targets over a $360°$ azimuth. Transmitted signals of TACAN is identified by three letter code transmission and is interlocked so that pilots using TACAN can be assured that signals being received are definitely

ISSN: 2414-1895 DOI: 10.6919/ICJE.202205_8(5).0090

from the same ground station. TACAN is "paired" in the frequency channel of each VORTOC facility, which can simplify take off operation. In addition, the rotating antenna is also used in the field of automatic driving. Automated driving uses a lidar system with a rotating antenna. The lidar system can scan the vehicle body $360°$ to draw a high-resolution topology around the vehicle. However, the applications of these rotating antennas are different from those of this paper. This paper can better simulate and observe the changes of wireless communication frequency through DAIA system.

2. System model

In this section, we present the operation of a wireless communication network that uses IA for the uplink. We assume a scenario with 2 source node S_k, $\forall k \in \{1,2\}$ and two destination nodes D_j, $\forall j \in \{1,2\}$ which are equidistant. Each source node sends two independent signals $W_{k,j}$ to the receiving node through X channel. All nodes are in each other's range, two independent messages are sent on different bandwidths and use OFDM with 3N subcarriers. As a baseline, each node has only single antenna. Note that, all nodes are fixed, but the rotation speed of the antenna is variable. In the following system, we assume that Doppler is only affected by the relative movement of transmitting and receiving ends, not by the environment.

We simulate the relative movement between the transmitting node and the receiving node by changing the rotation speed of the antenna. The Doppler shift between the transmitter of the S^{th} node and the receiver of the D^{th} node is:

$$f_d^{k,j} = \frac{v_{k,j} cos\varphi_{k,j} cos\phi_{k,j}}{c} f_c \tag{1}$$

where $v_{k,j}$ is the relative moving speed between the transmitter of the S^{th} node and the receiver of the D^{th} node. Here, we only consider the case where one node moves. If both nodes move, $v_{k,j}$ represents the relative speed between nodes. c is the propagation speed of underwater sound. $\phi(k,j)$ and $\varphi(k,j)$ denote, respectively, the angle between the transmit beam direction of the transmitter in the S^{th} node and the receive beam direction of the receiver in the D^{th} node. For instance, the arrival angles, $\phi(k,j)$ of the sending node are measured with respect to the direction of OA or OB (see Fig. 1-(b)). The incident angle of the transmission point is $\angle AOB$, Point B is horizontal, so the incident angle of point B is 0.

2.1 Transmit Signal Model

We consider an OFDM communication frame consisting of M symbols, each of which has a total bandwidth of $N\Delta f = B$. Here, T_{cp} and T denote, respectively, the cyclic prefix (CP) duration and the elementary symbol duration, $\Delta f = 1/T$ is the subcarrier spacing, and N is the number of subcarriers. Then, the complex baseband transmit signal for the m^{th} symbol is given by:

$$s_{k,m}(t) = \frac{1}{\sqrt{N}} \sum_{n=0}^{N-1} x_{n,m} e^{j2\pi n \Delta f t} \tag{2}$$

where $x_{n,m}$ denotes the complex data symbol on the n^{th} subcarrier for the m^{th} symbol. Two sending nodes send two independent messages respectively, including a desired message and an interference message, so the transmitted signal over the block of M symbols for node S_1 can be written as:

ISSN: 2414-1895 DOI: 10.6919/ICJE.202205_8(5).0090

$$X_{S_1} = \sum_{m=0}^{M-1} s_{k,m}(t) e^{j2\pi f_{\{c,W_{1j}\}} t} \tag{3}$$

where $f_{\{c,W_{1j}\}}$ denotes the carrier frequency of message $W_{k,1j}$.

The frequency domain channel fading matrix H_{kj} is a diagonal matrix whose diagonal entries are the Fourier transform of the time domain channel impulse responses (CIRs) $h_{kj}[n]$. $h_{kj}[n]$ is modeled by a tapped delay line model:

$$h_k j[n] = \sum_{M=0}^{N_{kj}} \alpha_{kj}[m] \tag{4}$$

where N_{kj} denotes the number of significant taps in $h_{kj}[n]$. We assume that all the terms $\alpha_{kj}[m]$ are independent zero-mean complex Gaussian with non-identical variances.

2.2 Receive Signal Model

As shown in Fig. 2, two sending nodes and two receiving nodes are directly equidistant. Each transmitting node sends two independent messages by different carriers without mutual interference, so the receiving node D1 accepts four messages in different frequency bands.

$$Y_{D_1}(K) = H_{j,k}(K) X_{j,k}\left(K - \frac{f_{c,W_{jk}}}{\Delta f}\right) + E(K) \tag{5}$$

where $E(K)$ is the noise component. In our model, Noise can be ignored because we focus on the DoF, which is available in high SNR region. The receivers do not consider the influence of time delay.

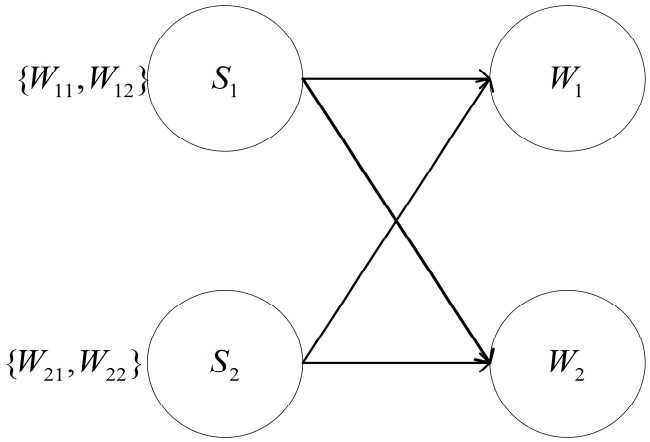

Fig. 2 System model of the 2 × 2 X channels.

3. Frequency domain interference alignment scheme

The two transmitting nodes send four messages in four different frequency bands. We expect to change the receiving frequency band of interference messages by adjusting the Doppler shift of transmitting nodes and receiving nodes. Define the frequency shift matrix as:

ISSN: 2414-1895 DOI: 10.6919/ICJE.202205_8(5).0090

$$D(f_d^{k,j}) = \begin{bmatrix} 1 & 0 & \cdots & 0 \\ 0 & e^{j\frac{2\pi f_d^{k,j}}{N\Delta f}} & \cdots & 0 \\ \vdots & \vdots & \ddots & \vdots \\ 0 & 0 & \cdots & e^{j\frac{2\pi f_d^{k,j}}{N\Delta f}(N-1)} \end{bmatrix} \tag{6}$$

where $f_d^{k,j}$ stands for the Doppler shift received by sending message W_{kj} and vectors as:

$$\begin{cases} X_{jk} = [X_{jk}(0), X_{jk}(1), \ldots, X_{jk}(N-1)]^T \\ Y_{jk} = [Y_{jk}(0), Y_{jk}(1), \ldots, Y_{jk}(N-1)]^T \end{cases}$$

where $[\cdot]^T$ stands for transpose, and $Y(K) = FFT\{y(n)\}$.

3.1 The Effects of Antenna Rotation Speed

Conventionally, the antenna is fixed ($v = 0$), but as rotation speed increases, two conflicting phenomena happen. We can more easily explain this conflict through a single carrier, as shown in the Fig. 3, The Fig. 3-(a) shows an illustration of the single-sided magnitude response of $r_1(t)$, $r_2(t)$, $h_1(t)$ and $h_2(t)$. When $v = 0$, $H_1(f)$ and $H_2(f)$ are just impulses, and have no relevant effect on $r_1(f)$ and $r_2(f)$. However, as v increases, $H_1(f)$ and $H_2(f)$ tend to move as shown in Fig. 3-(b). Due to the influence of Doppler shift, $H_1(f)$ and $H_2(f)$ gradually move away from zero frequency. On the other hand, $Y(f) = H(f) \otimes R(f)$, $Y(f)$ also tend to move as shown in Fig.4-(c). $\otimes$ denotes the convolution operator. As a result of frequency shift, by controlling the rotation speed of sending nodes 1 and 2, we make the messages sent by 1 and 2 accept at different frequencies. Based on this theory, we give different alignment schemes.

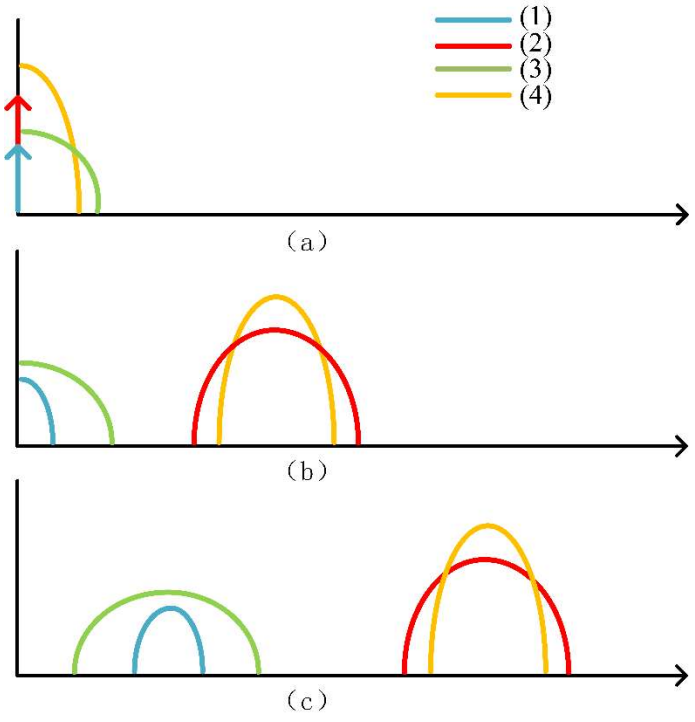

Fig. 3 Illustrations of magnitude responses of (1) $R_1(f)$, (2) $R_2(f)$, (3) $H_1(f)$ and (4) $H_2(f)$ which are Fourier transforms of $r_1(t)$, $r_2(t)$, $h_1(t)$ and $h_2(t)$ respectively.

ISSN: 2414-1895 DOI: 10.6919/ICJE.202205_8(5).0090

3.2 General Case I: The Sending Nodes Move and the Receiving Nodes are Fifixed

Firstly, we analyze the situation that the receivers are relatively stationary ($v=0$) and the transmitters are relatively moving. Generally, nodes s_1 and s_2 send two independent messages at different speeds, that is multiply the sending node by different frequency offset matrices. So we can get:

$$X_{S_1}=e^{-j2\pi f_d^{11}t}\sum_{m=0}^{M-1}s_{k,m}(t)e^{j2\pi f_{c,11}t}+e^{-j2\pi f_d^{12}t}\sum_{m=0}^{M-1}s_{k,m}(t)e^{j2\pi f_{c,12}t} \tag{7}$$

$$X_{S_2}=e^{-j2\pi f_d^{21}t}\sum_{m=0}^{M-1}s_{k,m}(t)e^{j2\pi f_{c,21}t}+e^{-j2\pi f_d^{22}t}\sum_{m=0}^{M-1}s_{k,m}(t)e^{j2\pi f_{c,22}t} \tag{8}$$

Here, node s_1 and node s_2 frequency offset matrix is different. The receiving node D_1 in (4) can be expressed as:

$$\begin{aligned}Y_{D_1}(K)=&D(f_d^1)H_{1,1}(K)X_{1,1}\left(K-\frac{f_{c,11}}{\Delta f}\right)\\&+D(f_d^1)H_{1,2}(K)X_{1,2}\left(K-\frac{f_{c,12}}{\Delta f}\right)\\&+D(f_d^2)H_{2,1}(K)X_{2,1}\left(K-\frac{f_{c,21}}{\Delta f}\right)\\&+D(f_d^2)H_{2,2}(K)X_{2,2}\left(K-\frac{f_{c,22}}{\Delta f}\right)\end{aligned} \tag{9}$$

After proper adjustment of nodes s_1 and s_2 speed, the alignment conditions for interference messages W_{12} and W_{21} is given by:

$$f_{c,12}+f_d^1=f_{c,21}+f_d^2 \tag{10}$$

It should be noted that the minimum unit of frequency offset here is the subcarrier interval, that is $f_c=N\Delta f$, N is a positive integer. In this case, we only need to adjust the speed of one node to align the interference messages to the same frequency band. Through the speed adjustment of condition (10), we can send signals in four frequency bands and receive signals in three frequency bands.

$$\begin{aligned}Y_{D_1}(K)=&H_{1,1}(K)X_{1,1}\left(K-\frac{f_{c,11}+f_d^1}{\Delta f}\right)\\&+H_{2,2}(K)X_{2,2}\left(K-\frac{f_{c,22}+f_d^2}{\Delta f}\right)\\&+\gamma\tilde{H}(K)\tilde{X}\left(K-\frac{\tilde{f}_c}{\Delta f}\right)\end{aligned} \tag{11}$$

ISSN: 2414-1895 DOI: 10.6919/ICJE.202205_8(5).0090

where γ stands for gain generated when interference signals W_{12} and W_{21} are aligned, $\tilde{H}$ represents the aligned channel and $\tilde{f}_c$ represents the frequency of the new subcarrier after alignment. Similarly, we can also get the reception of node D_2.

3.3 General Case II:All Nodes Move

Different from case I, the relative motion of all nodes is more in line with the characteristics of wireless communication. The senders are the same as (7) and (8), no different from case 1. The main change is at the receiving nodes.

$$\begin{aligned}\tilde{Y}_{D_1} &= D(f_d^{D_1})Y_{D_1}(K) \\ &= D(f_d^{D_1})D(f_d^{k,j})H_{j,k}(K)X_{j,k}\left(K-\frac{f_{c,W_{jk}}}{\Delta f}\right)\end{aligned} \tag{12}$$

$$\begin{aligned}\tilde{Y}_{D_2} &= D(f_d^{D_2})Y_{D_2}(K) \\ &= D(f_d^{D_2})D(f_d^{k,j})H_{j,k}(K)X_{j,k}\left(K-\frac{f_{c,W_{jk}}}{\Delta f}\right)\end{aligned} \tag{13}$$

where $\tilde{Y}$ represent receiver affected by Doppler. In our model, all antennas rotate in the same direction. Therefore, the frequency offset and frequency offset at the receiver have the opposite effect. From this, we can get:

$$\begin{aligned}\tilde{Y}_{D_1} = {} & H_{1,1}(K)X_{1,1}\left(K-\frac{f_{c,11}+f_d^1-f_d^{D_1}}{\Delta f}\right) \\ & + H_{1,2}(K)X_{1,2}\left(K-\frac{f_{c,12}+f_d^1-f_d^{D_1}}{\Delta f}\right) \\ & + H_{2,1}(K)X_{2,1}\left(K-\frac{f_{c,21}+f_d^2-f_d^{D_2}}{\Delta f}\right) \\ & + H_{2,2}(K)X_{2,2}\left(K-\frac{f_{c,22}+f_d^2-f_d^{D_2}}{\Delta f}\right)\end{aligned} \tag{14}$$

Due to the movement of the receiver, we should not only consider the frequency offset of the interference signal, but also consider that the expected signal is not disturbed. According to (14), We derive the conditions.

$$\begin{cases} f_{c,12}+f_d^1-f_d^{D_1}=f_{c,21}+f_d^2-f_d^{D_2} \\ f_{c,11}\le f_{c,21}-N\Delta f \\ f_{c,22}\le f_{c,12}+N\Delta f \end{cases} \tag{15}$$

The first condition in (15) is to align the interference signal to the same frequency band. Remaining conditions are to prevent the superposition of the desired signal due to the frequency offset generated by the receiving nodes. By adjusting the speed of each node, we can get the following at receiver D_1:

ISSN: 2414-1895 DOI: 10.6919/ICJE.202205_8(5).0090

$$Y_{D_1}(K) = H_{1,1}(K)X_{1,1}\left(K - \frac{f_{c,11} + f_d^1 - f_d^{D_1}}{\Delta f}\right) + H_{2,2}(K)X_{2,2}\left(K - \frac{f_{c,22} + f_d^2 - f_d^{D_2}}{\Delta f}\right) + \epsilon\tilde{H}(K)\tilde{X}\left(K - \frac{\tilde{f}_c}{\Delta f}\right) \tag{16}$$

4. Feasibility Analysis of DAIA

Since case 1 and case 2 are similar, we only use case 1 to analyze the feasibility of frequency domain alignment.

Consider the received signals at Receiver node 1. The desired signals arrive along the N vectors $H_{11}X_{11}$ and $H_{22}X_{22}$ while the interference arrives along the N vectors $H_{12}X_{12}$ and $H_{21}X_{21}$. Since:

$$D(f_d^1)H_{1,2}X_{1,2} = D(f_d^2)H_{2,1}X_{2,1} \tag{17}$$

it suffices to show that the $3N \times 3N$ matrix of two desired signals and one interference signals:

$$[D(f_d^1)H_{1,1} \quad D(f_d^1)H_{1,2} \quad D(f_d^2)H_{2,2}] \tag{18}$$

Multiplying (16) by the full-rank matrix $D^{-1}(f_d^1)$, we need to show that the matrix S, which is defined as:

$$S \doteq [H_{1,1} \quad H_{1,2} \quad D^{-1}(f_d^1)D(f_d^2)H_{2,2}] \tag{19}$$

Since $|S| = 0$ is equivalent to:

$$|FS| = 0 \tag{20}$$

where F is the inverse Fourier transform operator.

Since the diagonal entries of the diagonal matrix $H_{j,k}$ are independent, and it is known from (6) that the frequency offset matrix is also a diagonal matrix, we obtain that the probability of $|S| = 0$ is zero. Thus, the DAIA scheme is feasible.

5. Conclusion

The current paper has introduced, and studied a new class of systems termed as Doppler assisted interference alignment. The proposed class of systems employs rotating drum antennas, and exploits Doppler effect for interference alignment. We analyze the Doppler situation of the transmitting node and the receiving node in two different states, and use the Doppler frequency shift to successfully send messages in four frequency bands and receive messages in three frequency bands based on X channel. The results show that DAIA can be further extended from 2×2 to general M×N XC in frequency domain.

Acknowledgments

This research was funded by the Innovation Program of Shanghai Municipal Education Commission of China under Grant 2021-01-07-00-10-E00121 and the Natural Science Foundation of Shanghai under Grant 20ZR1423200.

ISSN: 2414-1895 DOI: 10.6919/ICJE.202205_8(5).0090

References

[1] V. R. Cadambe and S. A. Jafar, "Interference Alignment and Spatial Degrees of Freedom for the K User Interference Channel," 2008 IEEE International Conference on Communications, 2008, pp. 971-975, doi: 10.1109/ICC.2008.190.

[2] Q. Zhang, Q. Yong, J. Qin and A. Nallanathan, "On the Feasibility of the CJ Three-User Interference Alignment Scheme for SISO OFDM Systems," in IEEE Communications Letters, vol. 18, no. 2, pp. 309-312, February 2014, doi: 10.1109/LCOMM.2013.123113.132440.

[3] F. Liu, S. Jiang, S. Jiang and C. Li, "DoF Achieving Propagation Delay Aligned Structure for $K \times 2$ X Channels," in IEEE Communications Letters, vol. 21, no. 4, pp. 897-900, April 2017, doi: 10.1109/ LCOMM.2017.2647798.

[4] Feng L , Shuping W , Shengming J . Propagation-delay based interference alignment with extra time-slot for 3×3 X channel[J]. Application of Electronic Technique, 2019.

[5] O. El Ayach, A. Lozano and R. W. Heath, "On the Overhead of Interference Alignment: Training, Feedback, and Cooperation," in IEEE Transactions on Wireless Communications, vol. 11, no. 11, pp. 4192-4203, November 2012, doi: 10.1109/TWC.2012.092412120588.

[6] L. Wu, Z. Zhang, J. Dang and Y. Wu, "Frequency-Domain Intergroup Interference Coordination for V2V Communications," in IEEE Signal Processing Letters, vol. 24, no. 11, pp. 1739-1743, Nov. 2017, doi: 10.1109/LSP.2017.2757529.

[7] Y. Li, X. Lei, P. Fan and D. Chen, "Joint Iterative Interference Alignment and SCMA Technique for MIMO-OFDM Systems," 2016 IEEE 83rd Vehicular Technology Conference (VTC Spring), 2016, pp. 1-5, doi: 10.1109/VTCSpring.2016.7504308.

[8] J. M. Hamamreh, Z. E. Ankarali and H. Arslan, "CP-Less OFDM With Alignment Signals for Enhancing Spectral Efficiency, Reducing Latency, and Improving PHY Security of 5G Services," in IEEE Access, vol. 6, pp. 63649-63663, 2018, doi: 10.1109/ACCESS.2018.2877321.

[9] S. Park, M. Kim and Y. Ko, "Resource allocation for spatial-frequency domain based interference alignment scheme in MIMO-OFDM systems," 2014 IEEE International Conference on Communications (ICC), 2014, pp. 5753-5758, doi: 10.1109/ICC.2014.6884239.

[10] S. A. Shilo and Y. B. Sidorenko, "Variable Beam Width MMW Band Antenna," 2007 International Kharkov Symposium Physics and Engrg. of Millimeter and Sub-Millimeter Waves (MSMW), 2007, pp. 696-698, doi: 10.1109/MSMW.2007.4294781.

[11] J. Lorenzo et al., "Next generation of multi beam rotating antenna on SWIM scatterometer," 2010 IEEE International Geoscience and Remote Sensing Symposium, 2010, pp. 3478-3481, doi: 10.1109/ IGARSS. 2010.5649336.

[12] R. Jabeen and G. S. Tripathi, "Realization of Printed Rotated Slot Antenna With Tuning Stubs Fed by Microstrip Feedline for Bandwidth Enhancement," 2018 3rd International Conference On Internet of Things: Smart Innovation and Usages (IoT-SIU), 2018, pp. 1-4, doi: 10.1109/IoT-SIU.2018.8519844.

[13] D. A. Basnayaka, "The Aspects of Doppler Assisted Wireless Communication," 2019 14th Conference on Industrial and Information Systems (ICIIS), 2019, pp. 157-162, doi: 10.1109/ICIIS47346.2019.9063260.

[14] D. A. Basnayaka and T. Ratnarajah, "Doppler Effect Assisted Wireless Communication for Interference Mitigation," in IEEE Transactions on Communications, vol. 67, no. 7, pp. 5203-5212, July 2019, doi: 10.1109/TCOMM.2019.2912193.

[15] D. A. Basnayaka, H. Haas and T. Ratnarajah, "Doppler Effect Assisted Interference Mitigation for Wireless Communication," 2018 IEEE Global Communications Conference (GLOBECOM), 2018, pp. 206-212, doi: 10.1109/GLOCOM.2018.8647239.